Hydrogen Radicals, Nitrogen Radicals, and the Production of Ozone in the Middle and Upper Troposphere

P.O. Wennberg*, T.F. Hanisco, L. Jaeglé, D.J. Jacob, E.J. Hintsa, E.J. Lanzendorf, J.G. Anderson, R.-S. Gao, E.R. Keim, S.G. Donnelly, L.A. Del Negro, D.W. Fahey, S.A. McKeen, RJ. Salawitch, C.R. Webster, R.D. May, R.L. Herman, M.H. Proffitt, J.J. Margitan, E.L. Atlas, S.M. Schauffler, F. Flocke, C.T. McElroy, T.P. Bui

For Submission to Science, 1997

* to whom correspondence should be addressed.

P.O. Wennberg, T.F. Hanisco, E.J. Hintsa, E.J. Lanzendorf, J.G. Anderson, Harvard University, Department of Chemistry and Chemical Biology and Department of Earth and Planetary Sciences, 12 Oxford St., Cambridge,MA02138 email: wennberg@huarp.harvard.edu

L. Jaeglé, D.J. Jacob, Harvard University, Department of Earth and Planetary Sciences, 29 Oxford St., Cambridge, MA 02138

R.-S. Gao, E.R. Keim, S.G. Donnelly, L.A. Del Negro, D.W. Fahey, S.A. McKeen, M.H. Proffitt, NOAA Aeronomy Laboratory, 325 Broadway, Boulder CO 80303

R.J. Salawitch, C.R. Webster, R.D. May, J.J. Margitan, Jet Propulsion Laboratory, California Institute of Technology, 4800 Oak Grove Drive, Pasadena,CA91109

R.L. Herman, Department of Geology and Planetary Sciences, California Institute of Technology, 1200 E. California Blvd., Pasadena,CA91125

E.L. Atlas, F. Flocke, S.M. Schauffler, Atmospheric Chemistry Division, NCAR, 1850 Table Mesa Drive, Boulder, CO 80307

C.T. McElroy, ARQX, Atmospheric Environment Service, 4905 Dufferin Street, Downsview, Ontario, M3H 5T4, Canada

T.P. Bui, Ames Reseach Center, NASA, Moffett Field, CA 94035

Abstract. The concentrations of hydrogen radicals, OH and HO_2, in the middle and upper troposphere were measured simultaneously with those of NO, O_3, CO, H_2O, CH_4, non-methane hydrocarbons, and with the ultraviolet and visible radiation field. The data allow a direct examination of the processes that produce O_3 in this region of the atmosphere. Comparison of the measured concentrations of OH and HO_2 with calculations based on their production from water vapor, ozone, and methane demonstrate that these sources are insufficient to explain the observed radical concentrations in the upper troposphere. The photolysis of carbonyl and peroxide compounds transported to this region from the lower troposphere may provide the source of HO_x required to sustain the measured abundances of these radical species. The mechanism by which NO influences the production of O_3 is also illustrated by the measurements. In the upper tropospheric air masses sampled, the production rate for ozone (determined from the measured concentrations of HO_2 and NO) is calculated to be about 1 part per billion by volume each day. This production rate is faster than previously thought, and implies that anthropogenic activities that add NO to the upper troposphere, such as biomass burning and aviation, will lead to production of more O_3 than expected.

The hydrogen radicals OH and HO_2 (collectively known as HO_x) are central to the photochemistry of the troposphere (*1*). Although present at a mixing ratio of typically less than a few parts per trillion by volume (pptv), OH largely defines the oxidative power of the atmosphere (2). The oxidation of carbon monoxide (CO) and other hydrocarbons by OH is the dominant mechanism for the production of O_3 in the troposphere. It has been long assumed that the major source of HO_x in the lower atmosphere is the reaction of excited state oxygen atoms (produced in the photolysis of O_3) with H_20, with an important contribution from the oxidation of methane (CH_4). Photochemistry has been thought to be slow in the upper troposphere (defined here as the region between 8 km and the local tropopause) because the low concentration of H_2O was thought to preclude significant HO_x chemistry. It has been suggested, however, that the photolysis of acetone (3), hydrogen peroxide, HOOH (4), and methylhydrogen peroxide, CH_3OOH (5,6), transported from the lower troposphere can provide a significant source of HO_x in the upper troposphere.

We report here observations of OH and HO_2 in the upper troposphere. The measured concentrations of these radicals are significantly larger than would be expected on the basis of production from O_3, H_2O, and CH_4 alone. Inclusion of production of HO_x from the photolysis of acetone leads to much better agreement between calculated and observed HO_x. However, in air masses where there are indications of recent convective transport from the lower troposphere, observed concentrations of HO_x are often greater than calculated even when HO_x production from acetone is included. This finding is consistent with the theory that additional HO_x sources, such as peroxides, are important in the photochemistry of this region of the atmosphere.

These observations suggest that photochemistry in the upper troposphere has a much greater global significance than previously believed. The production of O_3 in this region is rapid, and this chemistry influences (he radiative balance at Earth's surface. These measurements directly illustrate that in the upper troposphere, the production rate of ozone increases rapidly with the concentration of NO. Thus, the presence of larger than expected concentrations of HO_x means that NO_x pollution emitted from aircraft will lead to the production of significantly more O_3 than calculated in recent modeling work (7).

Measurements

All observations were obtained between October 1995 and August 1996 with instruments aboard the NASA ER-2 aircraft (8). The flights were made near the airfields of operation: NASA-Ames Research Center, Mountain View, California (37°N, 122°W) and Barbers Point Naval Air Station, Hawaii (21 'N, 158°W). Typically, the ER-2 ascended quickly to 10 km before commencing a series of flight legs of 1/2 hour duration, staggered at approximately 2 km until maximum altitude was reached (21 km).

A key test of both the instrumentation and our understanding of atmospheric photochemistry is the measurement of the diurnal dependence of the concentration of the free radical species, OH, HO_2, and NO. Because these radicals are produced by photolytic processes, their concentration is expected to be negligible at night. On 3 August 1996, the ER-2 flew a series of flight legs near Hawaii beginning one hour prior to sunrise. In contrast to the other flights, the ER-2 maintained constant altitude (11.8 km) for many flight legs. The measured concentration of the hydrogen radicals, ([OH] and $[HO_2]$), were not statistically different from zero during the night (Fig. 1). This directly demonstrates that the ER-2 HO_x instrument does not suffer from artifacts that have hampered previous attempts to measure tropospheric OH with laser-based techniques (9).

We have used a photochemical model, constrained by the measured [NO], [CO], and the hydrogen radical precursors, $[O_3]$, $[H_2O]$, and $[CH_4]$ to calculate [OH] (*10*). Consistent with the observations, the calculated [OH] depends strongly on [NO] (Fig. 1). However, the absolute magnitude is significantly smaller than the measurements. The disagreement is largest at high solar zenith angles (sza). As will be discussed, the discrepancy is typical of upper tropospheric measurements and reflects the presence of primary HO_x sources in addition to the simple O_3, H_2O, and CH_4 photochemistry.

The catalytic cycling of HO_x and the production of O_3

The partitioning of the HO_x family between OH and HO_2 changes significantly as a function of altitude, reflecting important differences between the photochemistry of the stratosphere and the troposphere. In the lower stratosphere, the cycling of OH and HO_2 via reactions with O_3 represents an important catalytic pathway for O_3 destruction (*11*). In the upper troposphere, on the other hand, the low temperature, low mixing ratio of O_3 (< 150 parts per billion by volume (ppbv)), and high abundance of CO (> 50 ppbv)

completely change the impact of HO_x catalysis. HO_x cycling changes from being the major sink of O_3 in the lower stratosphere to the major source of O_3 in the upper troposphere:

$$OH + CO \xrightarrow{O_2} HO_2 + CO_2 \quad (1)$$

$$HO_2 + NO \longrightarrow OH + NO_2 \quad (2)$$

$$NO_2 + h\nu \longrightarrow NO + O \quad (3)$$

$$O + O_2 \longrightarrow O_3 \quad (4)$$

$$\text{Net: } CO + O_2 + O_2 \longrightarrow CO_2 + O_3.$$

Simultaneous measurements of [OH], $[HO_2]$, [NO], and [CO], combined with the measured rate coefficients for reactions 1 and 2 (*12*), provide a direct test of this photochemistry. The agreement between the measured and calculated ratio of $[HO_2]$ to [OH] in the upper troposphere is quite remarkable (Fig. 2), particularly given that the uncertainty in the rate of reaction 1 alone has been estimated to be nearly a factor of two (16) (*12*). The data suggest that the photochemical processes that cycle HO_x and lead to O_3 production (reactions 1 and **2)** are well understood. Provided that reactions 1 and 2 define the major pathway for cycling OH and HO_2, the rate of O_3 production will equal the rate of these reactions: $P_{O_3} = k_1 \times [OH] \times [CO] = k_2 \times [HO_2] \times [NO]$. To understand the production of O_3 in the upper troposphere we therefore need to understand what controls the absolute concentration of HO_x.

Sinks and Sources of HO_x in the upper troposphere

To test whether our understanding of the HO_x budget is complete, we calculate the rate of HO_x destruction (which can be inferred from the ER-2 measurements) and ask whether this sink can be balanced by known sources. We expect production and loss to balance because the lifetime of HO_x in the upper troposphere is relatively short (5-30 minutes).

HO_x Sinks

Individually, the lifetime of OH or HO_2 is seconds to minutes and is determined largely by the rates of reactions 1 and 2 which cycle OH and HO_2 rapidly. The lifetime of the HO_x family, however, is significantly longer and is determined by processes that eventually lead to the production of water vapor. The loss rate of HO_x can be estimated using the measurements of [OH], $[HO_2]$, [NO], and $[NO_y]$ (*13*), combined with calculated photolysis rates (*10*) and the measured kinetic rate constants (*12*).

The major processes that remove HO_x in the upper troposphere are:

$$OH + HO_2 \rightarrow H_2O + O_2 \quad (5)$$

$$HO_2 + HO_2 + M \rightarrow H_2O_2 + O_2 + M \quad (6)$$
$$OH + H_2O_2 \rightarrow H_2O + HO_2$$
$$\text{net: } OH + HO_2 \rightarrow H_2O + O_2$$

$$OH + NO_2 + M \rightarrow HNO_3 + M \quad (7)$$
$$OH + HNO_3 \rightarrow H_2O + NO_3$$
$$\text{net: } OH + OH + NO_2 \rightarrow H_2O + NO_3$$

$$HO_2 + NO_2 + M \rightarrow HNO_4 + M \quad (8)$$
$$OH + HNO_4 \rightarrow H_2O + NO_2 + O_2$$
$$\text{net: } OH + HO_2 \rightarrow H_2O + O_2$$

The competition between photolysis of H_2O_2, HNO_3, and HNO_4 and their reaction with OH determines the efficiency of HO_x removal for processes 6-8. From our measurements and the appropriate rate constants for these reactions (*12*), we estimate that process 5 accounts for more than 60 percent of the total loss rate of HO_x in most of the upper tropospheric air masses sampled. As a result, the sink depends quadratically on $[HO_x]$ and the photochemistry is strongly buffered.

Autocatalytic HO_x Sources

The concentrations of HO_x are partially maintained through the autocatalytic oxidation of hydrocarbons. For example, although OH is initially consumed in the oxidation of CH_4:

$$OH + CH4 \rightarrow CH_3 + H_2O, \quad (9)$$

subsequent chemistry leads to net HO_x production:

$$CH_3 + O_2 \rightarrow CH_3OO$$
$$CH_3OO + NO \rightarrow CH_3O + NO_2 \quad (10)$$
$$CH_3O + O_2 \rightarrow CH_2O + HO_2$$
$$CH_2O + h\nu \rightarrow H_2 + CO \quad (-2/3)$$
$$\xrightarrow{2O_2} 2\,HO_2 + CO \quad (-1/3)$$

When [NO] is sufficiently high (which is usually the case in the upper troposphere) almost two molecules of HO_2 are produced for each OH lost via reaction 9 (*14*). Although oxidation of other hydrocarbons also results in net production of HO_x, in the air masses sampled, the rate of CH_4 oxidation significantly exceeds the oxidation rate of all other hydrocarbons combined (*15*). From the measured [OH] and $[CH_4]$, we calculate that autocatalytic HO_x production is equal to approximately half of the calculated HO_x sink.

This source can only amplify other sources; without so-called primary sources of HO_x there would be no OH and hence autocatalytic production would not occur.

Primary Sources of HO_x

The reaction of excited state oxygen atoms, 0(1 D), with H_2O is usually considered to be the dominant mechanism for primary production of HO_x in the troposphere (2):

$$O_3 + h\nu \rightarrow O(^1D) + O_2$$
$$O(^1D) + H_2O \rightarrow OH + OH \qquad (11)$$
$$\text{net: } O_3 + H_2O + OH + OH + O_2$$

Recent measurements and analysis have greatly improved our understanding of the production of $O(^1D)$ from the photolysis of O_3. These studies indicate that throughout the troposphere and lower stratosphere, the 0(' D) production rate is larger than previously thought (*16*). Nevertheless, we calculate from the measured $[H_2O]$ and $[O_3]$ that process 11 can account for only a small fraction of the primary HO_x production required to balance the calculated sink of HO_x in many of the tropospheric air masses encountered above 10 km.

Recently Singh *et al. (3)* have suggested that the photolysis of acetone (*17*) can account for significant production of HO_x in the upper troposphere:

$$CH_3COCH_3 + h\nu \rightarrow CH_3CO + CH_3 \qquad (12)$$
$$CH_3CO + O_2 \rightarrow CH_3C(O)OO \qquad (13)$$
$$CH_3C(O)OO + NO \rightarrow CH_3 + CO_2 + NO_2 \qquad (14)$$

The subsequent chemistry of CH_3 (process 10) leads to production Of HO_2.

Acetone was not measured in our study. We have estimated the abundance of acetone from the measured [CO] using a correlation between these species observed in the upper troposphere on a previous aircraft campaign (*18*). From this relation, we estimate the concentration of acetone to be 300 pptv for the typical concentration of CO (70 ppbv). In the arid upper troposphere the production of HO_x from photolysis of this small concentration of acetone can be many times larger than the contribution from the reactions of $O(^1D)$ with H_2O.

Fig. 3 shows the calculated HO. production rate and the measured [OH] as the airplane descended into Barber's Point on the afternoon of 11 November 1995. The sza was 70 degrees. Between 10 and 15 km, the photolysis of acetone is calculated to produce nearly 5 times more HO_x than process 11. With the inclusion of the photolysis of acetone, the calculated [OH] increases by about a factor of two in the upper troposphere, improving agreement with the measurements, particularly above 10 km. The role of acetone is most pronounced when the sun is low in the sky (as in this descent) because the production rate of $O(^1D)$ from O_3 photolysis occurs at shorter wavelengths than acetone and thus is more strongly peaked at solar noon. As illustrated in Fig. 3 the 24-hour average HO_x

production rate from ozone photolysis (dashed **blue** line) is significantly larger than the rate calculated for the time of day of this descent. Thus for measurements made at high sun (low sza), particularly those made during the summer, we find that the agreement between calculated and measured $[HO_x]$ is less sensitive to the presence of acetone.

Even with the inclusion of acetone in our analysis, the calculated [OH] and $[HO_2]$ can sometimes be as much as a factor of 5 smaller than observed (6). This is particularly true of the measurements made during the winter. Early work by Chatfield and Crutzen and a more recent paper by Prather and Jacob suggest that convective transport of peroxides such as H_2O_2 (4) and CH_3OOH (5,6) may provide a large source of HO_x in the upper troposphere. Consistent with this theory, the largest differences between calculated and measured $[HO_x]$ are correlated with indicators of the recent convective origin of the air such as high relative humidity and elevated $[CH_3I]$ (a short-lived marker of transport from the planetary boundary layer) (6, 19). Recent HO_x measurements made from the NASA DC-8 aircraft also suggest that HO_x precursors are transported in convective events (20). While H_2O_2 is highly water soluble and should be scavenged efficiently in precipitation associated with convective updrafts, CH_3OOH is only sparingly soluble (*21*) and can therefore be transported over larger distances (22). Although the transport of CH_3OOH simply redistributes a HO_x reservoir from the lower to the upper troposphere, the impact on the photochemistry in the troposphere is significant because, as discussed below, the amount of O_3 produced per molecule of HO_x increases with altitude.

The lack of simultaneous measurements of acetone and peroxides leaves uncertainty in our inference of the species responsible for maintaining the large concentrations of HO_x measured in the upper troposphere. Further measurements during other seasons and at different locations are needed to investigate whether the conclusions about missing HO_x sources are robust globally. Simultaneous measurements of HO_x, acetone and the peroxides are clearly required. Nevertheless, the observations described here show that measured [OH] and $[HO_2]$ cannot be sustained by primary production from the reaction of $O(^1D)$ with H_20 alone (process 11). Photochemical models that include only this source of HO_x will significantly underestimate [OH] and $[H0_2]$ in the arid upper troposphere. It is likely that this underestimate of $[HO_x]$ is typical of the entire upper troposphere of the tropics and sub-tropics because the low temperature at and above 10 km generally restricts $[H_20]$ to less than 100 parts per million by volume (ppmv). Because the major primary source of HO_x in these air masses is not process 11, the rate of O_3 production does not, to first order, depend on either $[O_3]$ or $[H_2O]$.

HO., NO, and the 0_3 production efficiency

In our measurements, the mixing ratio of NO was usually between 50 and 200 pptv in the upper troposphere. This high concentration is not atypical; previous airborne measurements have shown that in the tropical and middle latitudes, [NO] usually increases with altitude (23). The elevated [NO] in the upper troposphere directly influences the efficiency of O_3 production. This efficiency is often described in terms of the NO chain length (the number of O_3 molecules produced before NO is converted to HNO_3). This is a

useful construct for the lower troposphere where most of the nitric acid is removed heterogeneously via rainout or dry deposition to the surface. In the upper troposphere, however, significant recycling of HNO_3 back to NO occurs via photolysis and reaction with OH. As a result, the NO chain length does not necessarily limit O_3 production.

The data presented here suggest that the primary sources of hydrogen radicals in much of the upper troposphere are the photolysis of transported HO_x precursors other than O_3 and H_2O. Thus, the O_3 production efficiency will, in part, be regulated by the HO_x chain length, (the number of O_3 molecules produced from these transported HO_x precursors). NO and NO_2 are the key species that determine this chain length. As discussed above, NO controls the partitioning within the HO_x family; the larger [NO], the smaller the ratio of $[HO_2]$ to [OH]. Increases in [NO] therefore lead to a faster rate of cycling within the HO_x family (reactions 1 and 2) with respect to the major HO_x sink (reaction 5), and as a result, more O_3 is generated from each molecule of HO_x before it is destroyed. In addition, increases in [NO] also accelerate autocatalytic production of HO_x (process 9 and 10) because this process depends on [OH], which is usually positively correlated with [NO] (Fig. 1). Thus we expect the HO_x chain length (and therefore the O_3 production rate) to increase rapidly with [NO].

The sensitivity of the production rate of O_3 to [NO] is illustrated by data obtained near San Francisco on 2 February 1996. On this flight, the ER-2 encountered an air mass with widely varying [NO] and only small changes in $[H_2O]$ (70 ± 15 ppmv), [CO] (95 ± 10 ppbv), and $[O_3]$ (60 ± 10 ppbv). The source of the NO may have been aviation exhaust, as numerous fresh plumes were observed with very high ratios of [NO] to $[NO_y]$ and small spatial extent (< 500 m). The non-plume observations illustrate the dependence of O_3 production on [NO]. For these calculations, the production rate of O_3, P_{O_3}, is assumed to equal the rate of reaction 2, $P_{O_3} = k_2 \times [HO_2] \times [NO]$, where k_2 is the rate coefficient for this reaction (*12*). For very low [NO] ($<1 \times 10^8$ mol cm^{-3}), the HO_x cycling occurs mostly via the self reaction of HO_2 followed by the photolysis of H_2O_2 and therefore, $[HO_2]$ is independent of [NO]. P_{O_3} is very low and increases linearly with [NO]. At larger [NO], $[HO_2]$ begins to decrease, and P_{O_3} increases more slowly than the rise in [NO].

The calculated response of $[HO_2]$ and P_{O_3} to variations in the primary production rate of HO_x (Fig. 4), shows clearly that the additional primary HO_x sources significantly increase P_{O_3}. For all calculated scenarios, P_{O_3} is predicted to be inversely correlated with [NO] for [N-O] $> 5 \times 10^9$ mol cm^{-3}, because processes 7 and 8 become important sinks of the hydrogen radicals leading to a reduction in the HO_x chain length. Additional atmospheric and laboratory studies detailing the photochemistry of HNO_3 and HNO_4 are required to understand better how P_{O_3} will vary at very high concentrations of NO.

The response of O_3 production to changes in [NO] illustrated in Fig. 4 is not generic: the response is larger when primary production of HO_x is enhanced. Furthermore, the level of NO for which the HO_x chain length begins to decrease depends on the ratio of $[NO_2]$ to [NO], which is strongly dependent on temperature and $[O_3]$ (*24*). For these flights, [NO]

in the upper troposphere increases with altitude and as a result, the HO_x chain length also increases. We calculate that the chain length typically increases from about 5 at ~7 km to 10-20 near the tropopause. This long chain length is important for O_3 production only because there is significant HO_x production in the upper troposphere fueled by acetone and other transported HO_x precursors. From the observations of $[HO_2]$ and [NO], we calculate about 1 ppbv of O_3 is produced each day in the upper tropospheric air sampled. In some air masses with very high [NO], P_{O_3} exceeded 5 ppbv per day.

Significance

The measured $[HO_x]$ suggests that in situ photochemistry occurring in the upper troposphere plays a much more important role than previously thought in determining the concentration of O_3. Limited observations of the change in tropospheric O_3 since pre-industrial times suggest that the increase in O_3 has contributed about 0.4 Wm^{-2} to the global mean radiative forcing at the surface (25). Because the O_3 changes have occurred mostly in the northern hemisphere, the forcing in this hemisphere may be twice as large. For comparison, the total increases in the global mean forcing from increases in the concentrations of long-lived greenhouse gases (such as CO_2, N_20, and CH_4) is estimated to be 2.45 $Wi^{n-}2$ (25). The measured $[HO_x]$, [CO], and [NO] are consistent with a photochemical production rate for O_3 of about 1 ppbv per day in the upper troposphere. Because the upper troposphere is flushed relatively quickly, the data suggest that chemistry occuring in this region may significantly affect the concentration of O_3 throughout the lower atmosphere.

References and Notes

1. H. Levy, II, *Planet. Space Sci.* **20, 919 (1972);** P.J. Crutzen, *Pure Appl. Geophys.* 106, 1385 (1973).; J.A. Logan M.J. Prather, S.C. Wofsy, M.B. McElroy, *J. Geophys. Res.* **86, 7210,(198 1);** D.H. Ehhalt, **H.-P. Drone, D. Pope,** *Proc. Royal Soc. Ed.* **97B**, 17 (1991).
2. D. Kley, *Science* 276, 1043 (1997).
3. H. Singh, *et al., Nature* **378, 50(1995).**
4. R.B. Chatfield and P.J. Crutzen, *J. Geophys. Res.* 89,7111 (1984).
5. M.J. Prather and D.J. Jacob, *Geophys. Res. Lett.*, in press (1997).
6. L. Jaeglé *et* al., *Geophys. Res. Lett.*, in press (1997).
7. G. Brasseur, J.-F. Müller, and C. Granier, *J. Geophys. Res.* **101, 1423 (1996).**
8. The data set described here was obtained during the Stratospheric TRacers of Atmospheric Transport (STRAT) campaign. The instrumentation complement is similar to that which has been flown previously. OH and HO_2 were measured by laser induced fluorescence [P.O. Wennberg *et al., Rev. Sci. Inst.* 65, 1858 (1994); P.O. Wennberg *et al., J. Atmos. Sci.* 52, 3413 (1995)]; NO and NO_y (*13*) by chemiluminescence [D. W. Fahey et al., *Nature* 363, 509 (1993)]; H_20 by photofragment spectroscopy [E.M. Weinstock *et cd., Rev. Sci. Inst.* 65, 3544 (1994)]; O_3 by absorption spectroscopy [M.H. Proffitt and R.J. McLaughlin, *Rev. Sci. Inst.*, 54 1719 (1983)]; CO and CH_4 by diode laser absorption spectroscopy [C.R. Webster, R.D. May, C.A. Trimble, R.G. Chave, J. Kendall, *Applied Optics 33,454 (1991)];* and hydrocarbons by gas chromatography [L.E. Heidt, J.F. Vedder, W.H. Pollock, R.A. Lueb, B.E. Henry, *J. Geophys. Res.* **94, 11599 (1989)]. Measurements of the** spectrally resolved radiation field were made with a ultraviolet-visible spectroradiometer [C.T. McElroy, *Geophys. Res. Lett.* **22, 1361 (1995)]. Aerosol** surface area was measured with a focused-cavity aerosol spectrometer [J. C. Wilson *et al., Science,* **261 1140 (1993)].**
9. C.C. Wang and L.I. Davis Jr., *Phys. Rev. Lett.,* **32**, 349 (1974); D.D. Davis, W. Heaps, T. McGee, *Geophys. Res. Lett. 3,* 331 (1976). G.P. Smith and D.R. Crosley, *J. Geophys. Res.,* **95, 16427 (1990);** M.K. **Dubey,** T.F. Hanisco, P.O Wennberg, J.G. Anderson, *Geophys. Res. Lett.* 23, 3215 (1996) provide more detail about the interference.
10. The photochemical model used in this work is described by L. Jaeglé *et al.* (6). For the analysis described here, [NO] is fixed in the model to match the observed abundance. Photolysis rates used in this study were computed using a six-stream radiative transfer model constrained by the observed O_3 column and albedo. The model reproduces the photolysis rate of NO_2 and $O_3(\rightarrow O(^1D))$ calculated from the measured spectrally-resolved radiance to within 10 and 30 percent, respectively. The model calculates the steady-state concentrations of 50 species, including HO_2, OH, H_2O_2, O^1D, CH_20, CH_3O, CH_3O_2, CH_3OOH, NO_2, NO_3, N_2O_5, HNO_2, HNO_4, HNO_3, and peroxyacetylnitrate (PAN).
11. R.C. Cohen *et al., Geophys. Res. Lett. 21, 2539 (1994);* P.O. Wennberg *et al., Science* 266,398 (1994).
12. W.B. DeMore *et al., Jet Propul. Lab. Publ. 97-4 (1997).*

13. The sum of reactive nitrogen species (NO_y) is the concentration of NO + NO_2 + NO_3 + 2 x N_2O_5 + $ClONO_2$ + nitric acid (HNO_3) + peroxynitric acid (HNO_4) + all organic nitrates such as PAN. It was measured on the ER-2 by the catalytic conversion of these species to NO. Some other molecules such as HCN and NH_3 can interfere with this technique [D.W. Fahey, C.S. Eubank, G. Hubler, F.C. Fehsenfeld, *J. Atmos. Chem.* **3**, *435 (1985);* D.A.V. Kliner, B.C. Daube, J.D. Burley, S.C. Wofsy, *J. Geophys. Res.* **102 10759 (1997)]. For the measurements** discussed here, the concentration of NO_y was sufficiently high and the sensitivity to these interferences was sufficiently low that the measurement of NO_y is not subject to significant error.

14. When the concentration of NO is low (< 50 pptv), the reaction of HO_2 with CH_3OO reduces the HO_x source from the oxidation of methane and other hydrocarbons.

15. Although the rate constant for OH reacting with CH_4, k_9, can be significantly slower than the rate constant for OH reacting with other hydrocarbons, the abundance of methane is so large (1.8 ppmv) that the rate of reaction 9 (k_9 x [CH_4] x [OH]) vastly exceeds that of the other hydrocarbons. For example, although OH reacts with propane 1000 times faster than with CH_4, the measured concentration of methane was typically 50,000 to 100,000 times greater than that of propane in the upper troposphere.

16. H.A. Michelsen *et al.*, *Geophys. Res. Left.* **21, 2227 (1994); K.** Takahashi, **Y.** Matsumi, M. Kawasaki, *J. Phys. Chem.* **100,** *4084 (1996);* E. Silvente, R.C. Richter, M. Zheng, E.S. Saltzman, A.J. Hynes, *Chem. Phys. Lett.* 264309 (1997); S.M. Ball, G. Hancock, S.E. Martin, J.C. Pinot de Moira, *ibid* 264531 (1997); R.K. Talukdar et *al., Geophys. Res. Lett. 241091* (1997).

17. S.A. McKeen *et al., Geophys. Res. Lett*, in press (1997).

18. The correlation of CO with acetone was determined from measurements of these species during the PEM-West (B) DC-8 campaign: Acetone (pptv) = 6.1 x CO (ppbv) - 127 (17). This relationship may not be robust given the large uncertainty in our understanding of the budget of acetone [H. B. Singh *et al., J. Geophys. Res.*, 99 1805 (1994)]. HO_x measurements during STRAT suggests that this relationship likely overpredicts acetone in the lower stratosphere. In the middle and upper troposphere, however, the Singh *et al.* data suggest a surprisingly small variation for acetone. The efficiency of acetone as a HO. source depends strongly on the ratio of NO to NO_2 because the reaction of $CH_3C(O)OO$ with NO_2 forming PAN competes with reaction 14. In the upper troposphere, because the ratio of NO to NO_2 is large and because it is readily photolyzed, PAN is calculated to be a relatively small fraction of the total NO_y (*17*).

19. I. Folkins *et al., Geophys. Res. Lett.*, in press (1997)

20. W.H. Brune *et al.,* accepted for publication, *Geophys. Res. Lett. (1997);* L. Jaeglé *et* d., accepted for publication, *Geophys. Res. Lett. (1997).*

21. D.W. O'Sullivan, M. Lee, B.C. Noone, B.G. Heikes, *J. Phys. Chem.* **100,** 3241 (1996).

22. Previous comparisons of calculated and observed concentrations of CH_3OOH in the upper troposphere are consistent with a large source of CH_3OOH from deep convection [D.J. Jacob *et al., J. Geophys. Res.,* **101** 24235 (1996)].

23. J. Bradshaw, S. Smyth, S.C. Liu, D.D. Davis, R.E. Newell, *Rev. Geophys.*, in press (1997).

24. During the daytime, NO and NO_2 are interconverted on a time scale of less than 2 minutes due to the fast photolysis rate of NO_2 (J_{NO2}). Assuming that the rate of photolysis of NO_2 is balanced by the reaction of NO with O_3 and HO_2 we can estimate that $[NO_2] = [NO] \times ((k_{O_3+NO})[O_3] + (k_{HO_2+NO})[HO_2] \} \div J_{NO_2}$.

25. Intergovernmental Panel on Climate Change, *Climate Change: Radiative Forcing of Climate Change: The Scientific Assessment* (Cambridge Univ. Press, New York, 1994); For more detail on the radiative effects of tropospheric ozone see J. Hansen, M. Sate, R. Ruedy *J. Geophys. Res.* **102, 6831 (1997);** A.A. Lacus, D.J. Wuebbles, J.A. Logan, *J. Geophys. Res.* 95,9971 (1990);

26. We thank the pilots and ground crew of the NASA ER-2 Aircraft. We thank the STRAT mission scientists, Steve Wofsy of Harvard University and Paul Newman of NASA GSFC, for their efforts in obtaining this data set. Kathy Wolfe, Jim Barrilleaux, Estelle Condon, Steve Hipskind, Michael Craig, Steven Gaines, Joe Goosby, and Quincy Allison provided excellent logistical support for this field effort. We acknowledge Richard Lueb, Verity Stroud, and Heidi Krapfl for their efforts on the whole air sampler data set. A portion of the research described in this paper was carried out by the Jet Propulsion Laboratory, California Institute of Technology, under contract with NASA. Partial support for analysis of the STRAT data set was provided by a grant from the National Science Foundation (ATM 9612282). The STRAT program was supported by NASA through the Upper Atmosphere Research and the Atmospheric Chemistry Modeling and Analysis Programs and by the Atmospheric Effects of Aviation Project, We thank the officers of these programs, Michael Kurylo, Howard Wesoky, Jack Kaye, Randall Friedl, , Dean Peterson, and Philip DeCola for their support.

Fig. 1. Sunrise measurements of NO (A) and OH (B). The measurements have been filtered with a 1-minute running median. A photochemical model, constrained by the observed abundance of NO, CO and long-lived species such as O_3 and H_2O, has been used to calculate OH. Although the structure in measured [OH] (driven by the variation in NO), is mirrored in the calculation (B, gray line), the absolute magnitude is significantly smaller. This model scenario assumes that the source of the hydrogen radicals is limited to simple O_3, H_20, and CH_4 photochemistry. At sunrise, the concentration of NO increases more rapidly than OH due to the rapid photolysis of its source, $N0_2$.

Fig. 2. The partitioning of HO_x in the upper troposphere. The processes which produce O_3 in the troposphere determine the ratio of $[HO_2]$ to [OH] (reactions 1 and 2). The agreement between the measured and calculated ratio is much better than could be expected given the uncertainty in the thermal rate coefficients (+120% - 70%) for these reactions and the measured ratio ($\pm$ 20%). For example, shown on this plot as dashed lines are the calculated ratios determined by adjusting the rate constant for reaction 1 to its 10 uncertainty limits (*12*). This figure includes data for which NO and OH are more than 10 times above their detection limit (50, and 0.25 pptv respectively). In addition, to sol ensure that the partitioning is not influenced by production or loss of HO_x, only data where the calculated HO, cycling rate is significantly faster than the calculated rate of HO_x destruction (and therefore HO_x production) is shown.

Fig 3. The production rate of HO_x (A) and the concentration of OH (B) on 7 November 1995. (A) As shown in blue, the HO_x production rate from the reaction of $O(^1D)$ with H_2O (process 11), drops by orders of magnitude between 7 km and the tropopause following the drop in the mixing ratio of H_2O. **Shown** in red is an estimate of the HO_x production rate from photolysis of acetone, which recent measurements have shown is ubiquitous in the upper troposphere. Both the instantaneous production rates (solid lines) and the 24-hour average rates (dashed lines) are shown. (B) Without the acetone source, the measured [OH], shown here filtered with a 30-sec running median, and $[H0_2]$ (not shown) are underpredicted by about a factor of 2 between 12 km and the tropopause. Even with acetone, $[HO_x]$ is often underpredicted. For example at the bottom of this profile, measured OH concentrations are 20-10070 larger than calculated. Typical of all the observations, the agreement between calculated and measured [OH] is excellent in the stratosphere.

519 Fig. 4. The relationship between O_3 production and NO. Measurements made on 2
520 February 1996 illustrate how the O_3 production rate depends on NO. At 240mb (10.7
521 km),large variability in NOwas observed. Numerous aircraft plumes with very high [NO]
522 (>1ppbv) were also sampled at this altitude. Because the photochemistry within the
523 plumes is far from photochemical equilibrium, only data obtained in the background
524 atmosphere are shown here. To exclude the plumes, the data was sorted for NO/NO_y c
525 0.3 and for times when the concentration of NO changed by less than 50 pptv per second
526 (corresponding to 210 m spatial extent). Three model curves illustrate how $[HO_2]$ (A)
527 and the O_3 production rate (B) vary as a function of assumptions about the production
528 rate of HO.. In blue, acetone is assumed to be zero; the primary HO_x source is limited to
529 production from the reaction of $O(^1D)$ with H_20. In red, acetone is assumed to be present
530 at 400 pptv (*18*). In green is shown a calculation where we have increased the primary
531 HO_x source to a value consistent with the HO_x observations. At very high [NO] the
532 calculations predict that O_3 production will be anticorrelated with [NO] because the HO_x
533 chain length becomes shorter as the large concentration of $N0_2$ increases the HO_x sink via
534 processes 7 and 8.
535

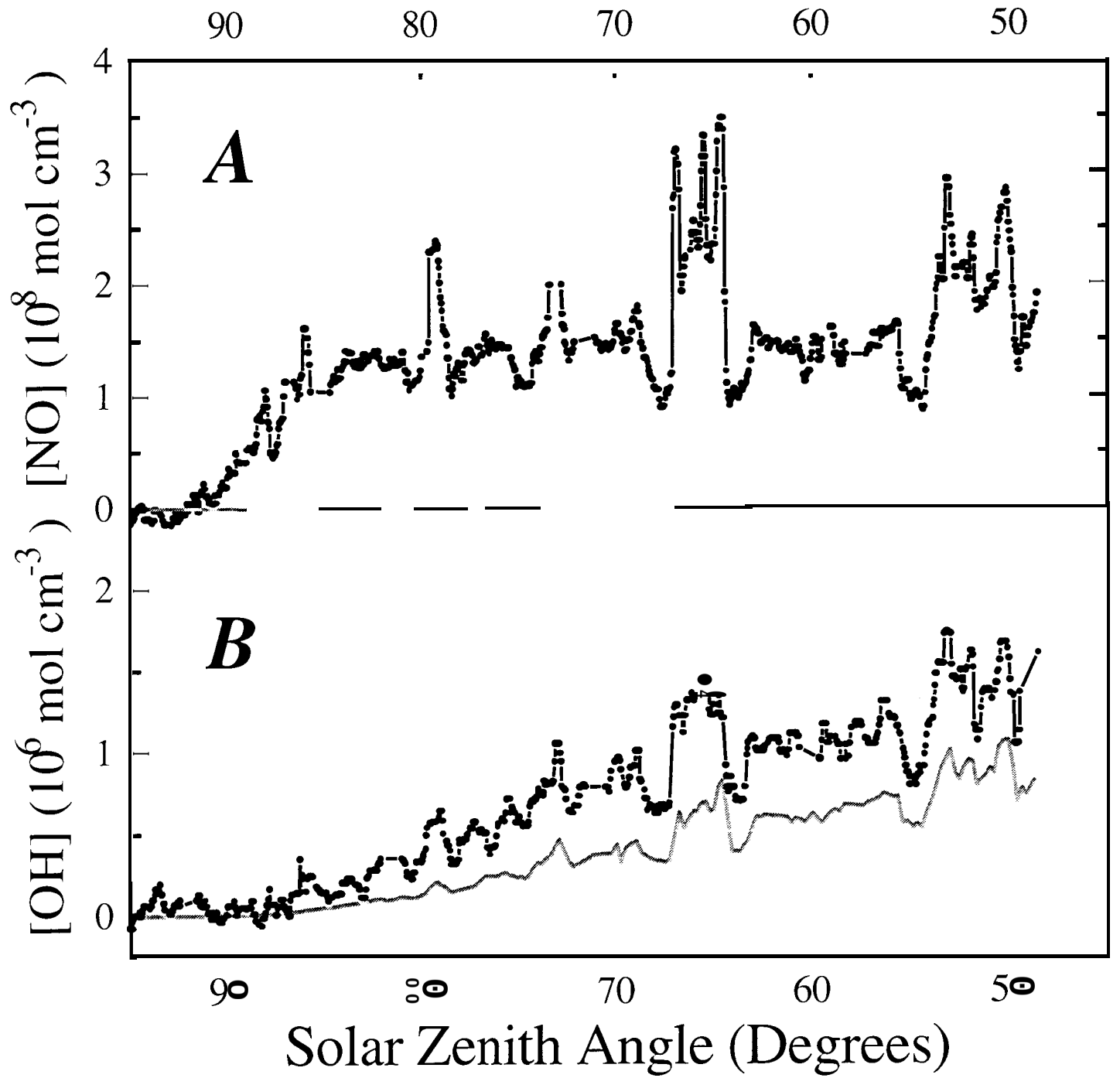
90
80
70
60
50
4
3
2
1
0
2
1
0
A
B
[NO] (10^8 mol cm^{-3})
[OH] (10^6 mol cm^{-3})
90
80
70
60
50
Solar Zenith Angle (Degrees)

Figure 1

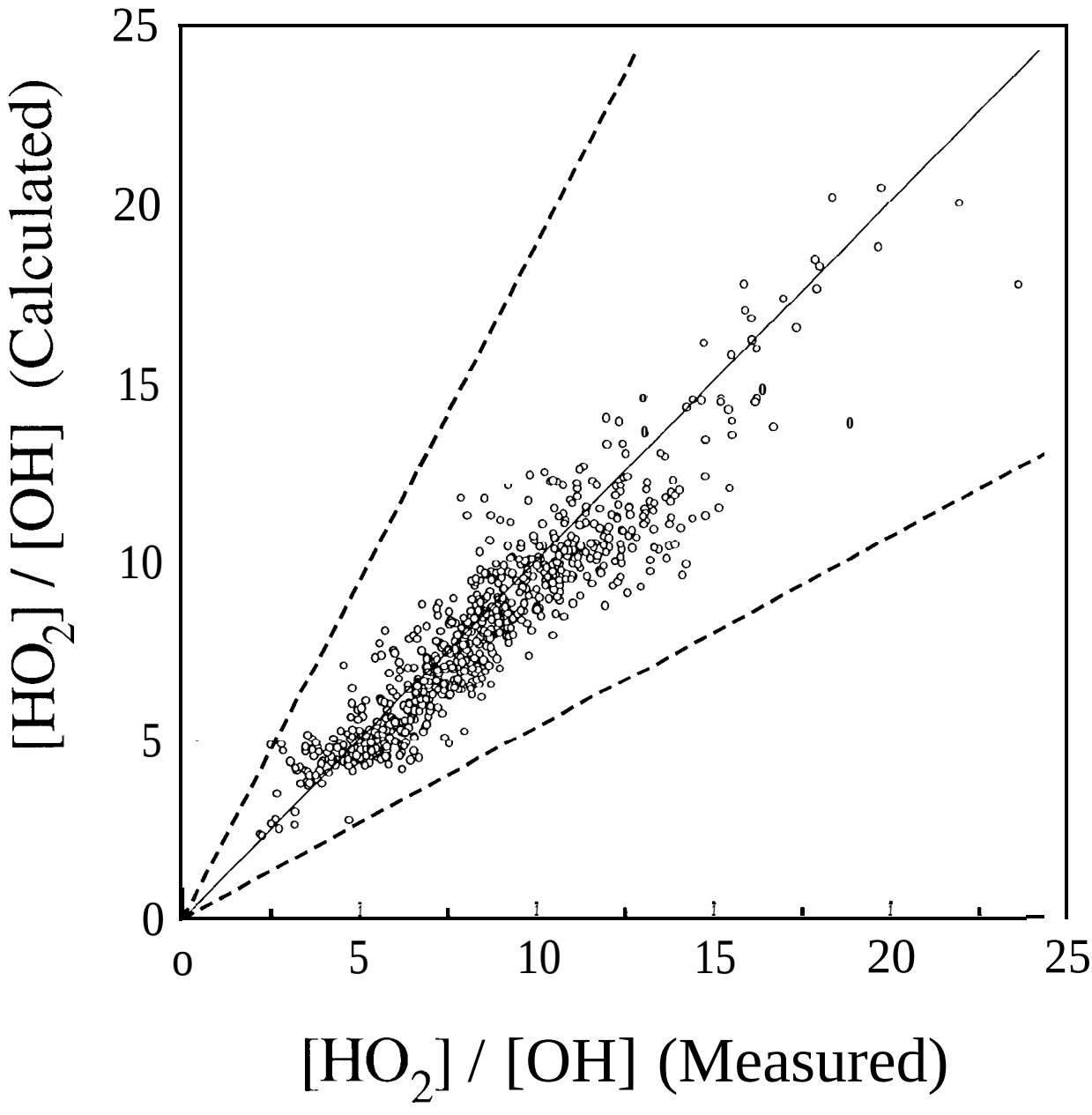

Figure 2

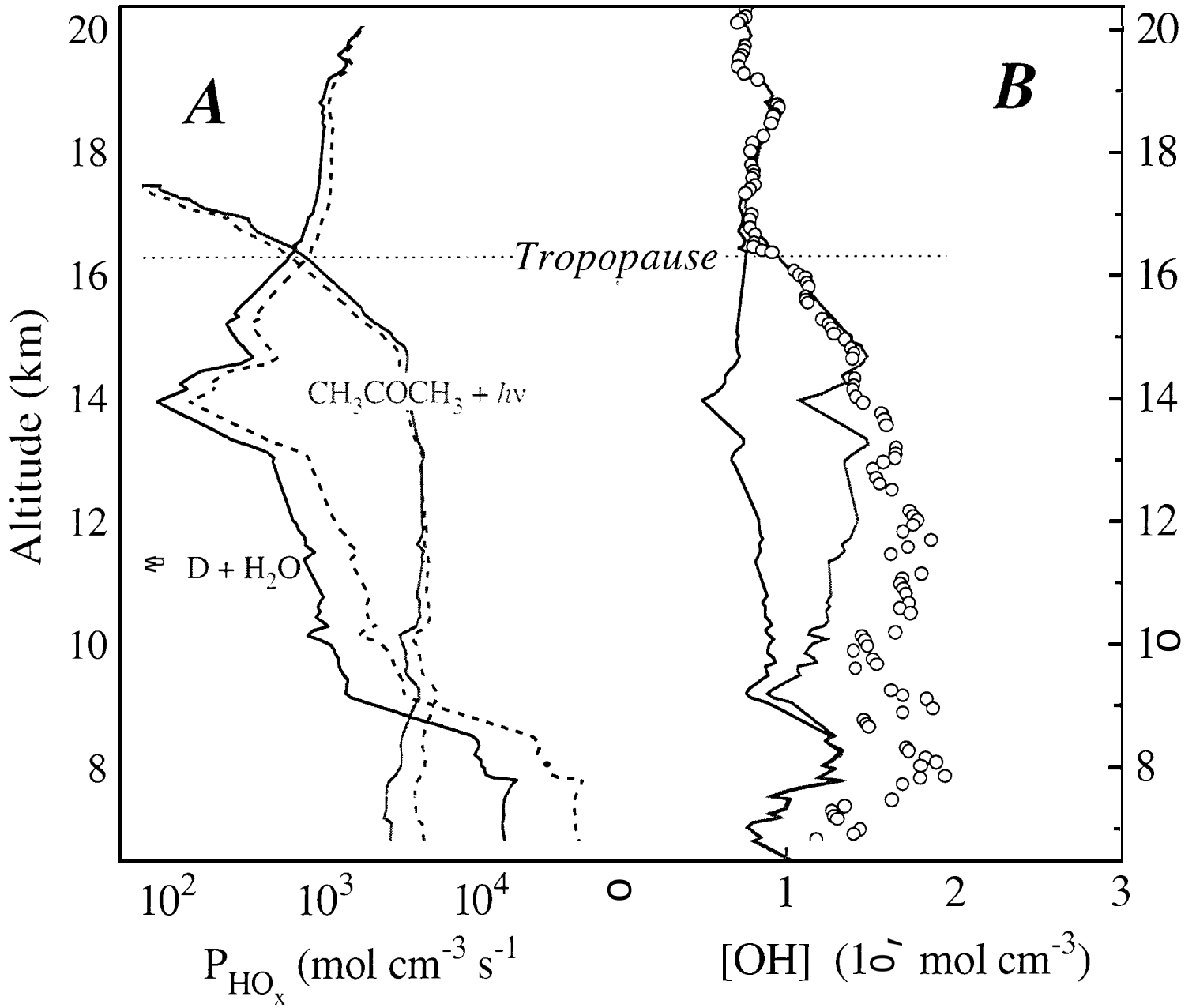
A
B
Tropopause
$CH_3COCH_3 + h\nu$
$O(^1D) + H_2O$
Altitude (km)
20
18
16
14
12
10
8
10^2
10^3
10^4
0
1
2
3
P_{HO_x} (mol cm^{-3} s^{-1})
[OH] (10^7 mol cm^{-3})

Figure 3

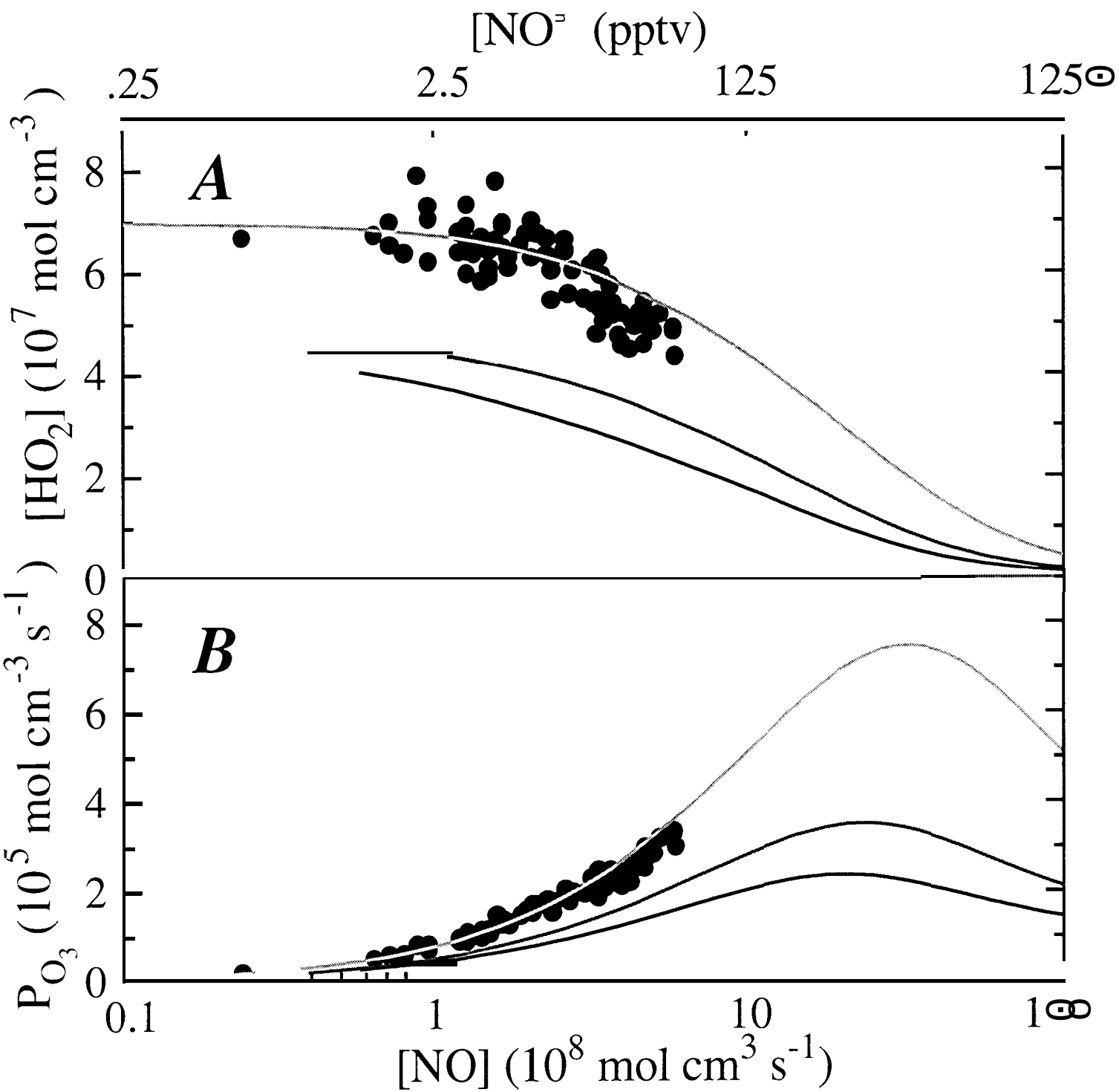
[NO] (pptv)
.25
2.5
125
1250
A
B
[HO2] (10^7 mol cm^-3)
P_O3 (10^5 mol cm^-3 s^-1)
0
2
4
6
8
0.1
1
10
100
[NO] (10^8 mol cm^3 s^-1)

Figure 4